Image Segmentation Using Gradient Vector Diffusion and Region Merging

Zeyun Yu and Chandrajit Bajaj
Department of Computer Science, University of Texas at Austin, Austin, Texas 78712, USA
{zeyun, bajaj}@cs.utexas.edu

Abstract

Active Contour (or Snake) Model is recognized as one of the efficient tools for 2D/3D image segmentation. However, traditional snake models prove to be limited in several aspects. The present paper describes a set of diffusion equations applied to image gradient vectors, yielding a vector field over the image domain. The obtained vector field provides the Snake Model an external force as well as an automatic way to generate the initial contours. Finally a region merging technique is employed to further improve the segmentation results.

1. Introduction

Since it was first proposed by *M.Kass etc.*[1], active contour (or snake) model has drawn a lot of attention from researchers in image-related fields. Due to its efficiency of converging to the desired features within an image by simply defining an energy function, snake model has found many applications such as edge detection, shape modeling, segmentation, and motion tracking (e.g., see [1, 3, 10]).

The traditional snake model [1] in 2D is defined by an energy functional:

$$E = \int_0^1 \frac{1}{2}[\alpha\|\mathbf{x}'(s)\|^2 + \beta\|\mathbf{x}''(s)\|^2] + E_{ext}(\mathbf{x}(s))ds. \quad (1)$$

where $\mathbf{x}(s) = [(x(s), y(s)]$, and $s \in [0, 1]$. The first two terms within the above integral stand for the internal force that is determined by the physical properties of the snakes, while the third term is viewed as the external force that is the main issue discussed in active contour models.

Generally there are several difficulties with this model. One is its sensitivity to the initial contours. Some techniques have been proposed to rectify this problem, e.g., *multi-scale method* [6], *distance potential force* [3], *inflating balloons* [7], and more recently, *gradient vector flow (GVF)* [2]. These techniques extend the external force to a much larger range over the image domain and thus reduce the sensitivity to the initial contours.

The second difficulty with the traditional model is that it is difficult for the snake to move into the boundary concavities. As we know, the internal force of a snake usually makes the snake as straight as possible. Thus, if the external force in (1) is not large enough to pull the snake into the boundary concavities, the snake will always stop near the "entrance" of the concavities. Although several approaches have been proposed to solve this problem (e.g., see [7, 3]), most of them do not give satisfying results. *Xu*'s GVF method [2] and its improved version [4] were originally proposed to remedy this problem but still did not work very well in the case of long and thin boundary concavities (see next section for details). Furthermore, it remains a problem to handle boundary "gaps" or low-contrast boundaries that are overwhelmed by the nearby high-contrast boundaries.

A third problem with the traditional snake model is the stopping criterion. As we know, this model stops with a snake corresponding to the global minimum of (1). Thus some time-consuming techniques, such as *simulated annealing* [11] or *dynamic programming* [10] are needed to avoid the problems caused by local minima. Furthermore, even in the case that the global minimum is achieved, the final solution is still highly dependent on the choice of initial parameters. A *dual-snake* technique [12] was used to reduce the dependence on the choice of parameters. Similarly we will use a *multiple-snake* scheme to achieve this goal.

In the present paper we propose a new type of anisotropic diffusion equations to obtain the *gradient vector field*, which not only provides us a good guess of the initial snakes but also generates an external force on each pixel in the image domain. Unlike the diffusion equations seen in [2, 4], our diffusion scheme is based on the magnitudes and orientations of the vectors. This strategy greatly improves the behaviors of the vector diffusion when dealing with boundary concavities or "gaps" that *Xu*'s method and even its improved version cannot solve efficiently. Our proposed *gradient vector diffusion (GVD)* scheme, coupled with the idea of *multiple-snake*, can correctly obtain an initial segmentation, and then a region merging approach is used to find the desired segmentation of the entire image. We shall also briefly describe the relationship between our GVD-based

approach and the classic watershed method [14].

We organize the paper as follows: in section 2 we describe how to generate a gradient vector field and demonstrate the difference between our GVD scheme and *Xu*'s method. Section 3 will discuss how the gradient vector field generated by our method can be applied to image segmentation. Then we shall present some segmentation results on various types of images in section 4. Finally in section 5, we conclude the paper.

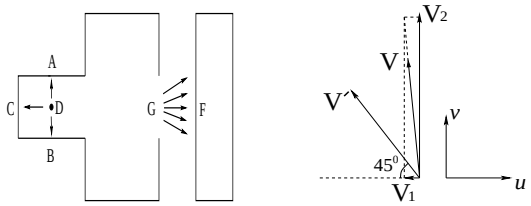

(a) Two problems with GVF *(b) Solutions*

Figure 1. Illustration of the problems and solutions. V and V' in (b) stand for the diffused vector by Xu's method and our method, respectively

2. Gradient Vector Diffusion

2.1. Previous Work and Analysis

In the work of *Xu etc.*[2, 4, 5], The following diffusion equations were used:

$$\begin{cases} \frac{du}{dt} = \mu\nabla^2 u - (u - f_x)(f_x^2 + f_y^2) \\ \frac{dv}{dt} = \mu\nabla^2 v - (v - f_y)(f_x^2 + f_y^2) \end{cases} \quad (2)$$

where (u, v) is initialized by $\nabla f(x, y)$ and $f(x, y)$ is an edge map of the original image: $f(x, y) = |\nabla I(x, y)|^2$.

This diffusion model was originally proposed to remedy the problem of the traditional snake model in case of boundary concavities (see fig.1(a) where ACB are shown). However, it does not work well when the boundary concavities are long and thin (see [4]). Then *Xu etc.* proposed a generalized version of this model, aiming to handle the long and thin concavities. Unfortunately even the generalized version (GGVF) still could not handle these cases efficiently. The reason is that, as shown in fig.1(a), the vectors propagated from C to D are very "weak" (with low magnitudes) while the vectors propagated from A and B to D are relatively much stronger, yielding the diffused vectors around D pointing either up or down. Another problem with both models is how to prevent the snakes from moving out of the boundaries "gap" or low-contrast boundaries near high-contrast boundaries as shown in fig.1(a) around point G.

2.2. Our Approach

Remember that GVF and GGVF apply the diffusion on Cartesian coordinate representation (u and v) of vectors. Actually, applying the diffusion on r (the magnitude of vector) and θ (the orientation of vector) can greatly improve the behaviors of the vector diffusion. Fig.1(b) shows how these two different ways diffuse two vectors and have totally different results. For the diffusion scheme based on r and θ, a very weak vector can largely affect a strong vector, both on its magnitude and on its orientation. This is the essential idea for our new diffusion approach. Furthermore, by using an anisotropic scheme, we can choose to weaken the orientation diffusion (as we will see in the following) if two vectors are pointing in almost opposite directions. Then the problem of boundary "gaps" can be easily solved.

Before we describe our diffusion equations, we shall give a definition of *sink*, which will be used in our algorithm:
Definition Given a vector field $\vec{\mathbf{v}}(i, j), i = 0, \cdots, m-1; j = 0, \cdots, n-1$, where m, n are the size of the image domain. The **sink** of a pixel A at (i, j), denoted by $sink(i, j)$, is defined as the total incoming amounts at A from all its neighbors minus the the magnitude of the vector at A.

In the following we will use different schemes to diffuse the vector magnitude r and orientation θ.

Our approach uses an anisotropic diffusion scheme [8] for the diffusion process of r:

$$\frac{dr}{dt} = \mu\nabla(s(\vec{\mathbf{v}}^{(0)})c_1(\|\nabla r\|)\nabla r) - h(r^{(0)})(r - r^{(0)}). \quad (3)$$

where

$$c_1(\|\nabla r\|) = e^{-\frac{\|\nabla r\|^2}{K^2}}, \quad h(r^{(0)}) = 1 - e^{-(r^{(0)}/K)},$$

and

$$s(\vec{v}(i, j)) = e^{-sink_+(i,j)},$$

where $sink_+(i, j)$ is equal to $sink(i, j)$ if $sink(i, j) \geq 0$. Otherwise it is equal to zero. In equation (3), $r^{(0)} = \|\vec{\mathbf{v}}^{(0)}\|$, where $\vec{\mathbf{v}}^{(0)}$ stands for the initial vector field that can be determined by ∇f. According to the definition, the *sink* is much larger around the boundary points than elsewhere. So $s(\vec{\mathbf{v}}^{(0)})$ can reduce the diffusion effect around boundary points while encouraging the diffusion elsewhere.

The diffusion equation for vector orientation θ plays an important role on making the vector field more "sensitive" to the boundary concavities but less "sensitive" around the boundary gaps. We shall assume that the orientations of the vectors are periodically defined on $(-\pi, \pi]$. The equation for vector orientation θ looks similar to (3):

$$\frac{d\theta}{dt} = \mu\nabla(s(\vec{\mathbf{v}}^{(0)})c_2(dif(\theta, \theta^*))dif(\theta, \theta^*)sign(\theta, \theta^*)) - h(r^{(0)})dif(\theta, \theta^{(0)})sign(\theta, \theta^{(0)})). \quad (4)$$

where θ^* is the orientation of one of the neighbors. $s(\vec{\mathbf{v}}^{(0)})$ and $h(.)$ are defined same as in (3). But $c_2(.)$ is different from $c_1(.)$ in (3):

$$c_2(x) = \begin{cases} e^{-\frac{2x}{\pi}} & \text{if } 0 \le x \le \frac{\pi}{2} \\ \frac{2}{\pi e}\frac{(x-\pi)^2}{x} & \text{if } \frac{\pi}{2} \le x \le \pi \end{cases}$$

This weighting function basically tells us that, if the difference of two vectors' orientations θ_1 and θ_2 is about $\pi/2$, then they can affect each other most significantly. But if the difference is a little bit greater than $\pi/2$, their influence to each other will rapidly decrease to zero.

In (4) we replace $\nabla\theta$ (as it should be in most anisotropic diffusion methods) with $dif(\theta, \theta^*)sign(\theta, \theta^*)$. The reason for this change is that in our case the orientation θ is periodically defined on $(-\pi, \pi]$. So the difference between two angles θ_1 and θ_2 can not be simply written as $\mid \theta_1 - \theta_2 \mid$, but should be the angle between the two corresponding vectors. And this angle could be positive or negative depending on the orientations of these two vectors. Therefore, the well-known *Maximum Principle* [8] in traditional heat diffusion scheme is no longer true in the case of orientation diffusion.

2.3. Comparison with Xu's Method

Fig.2(a) and *(b)* show the enlarged vector field near the boundary concavity (see fig.1(a) around ACB). It is clearly shown that, by our approach, the vectors in the concavity obviously changed their magnitudes and orientations and thus the snake can easily move into the bottom of the concavity. *Fig.2(c)* and *(d)* show the enlarged vector field near the boundary gap (see fig.1(a) around G). As we can see from *fig.2(c)*, traditional GVF has difficulty preventing the vectors near the boundary gap from being significantly influenced by the nearby boundaries, so that the snake may move out of the boundary gap. However, our approach can avoid this problem.

3. Image Segmentation

In this section we will briefly discuss how to apply the *gradient vector field* obtained by our approach to the image segmentation. As we have said before, the gradient vector field provides us an external force at each pixel as well as a way to generate the initial snakes.

3.1. Initialization of Snakes

There are several ways to choose the initial snakes (or seed points): by hand, by "balloons", or by the locus of the zero-crossing of the Laplacian of the smoothed images (see [9] for a summary). In our case, we will use the *source* points (defined later) as our seeds. The *source* points can be automatically generated from the gradient vector field.

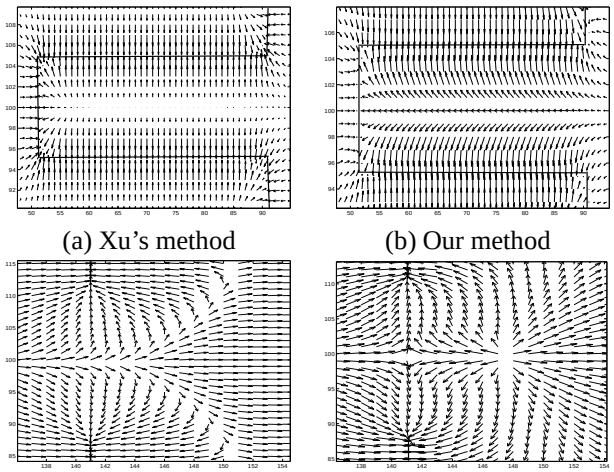

(a) Xu's method (b) Our method

(c) Xu's method (d) Our method

Figure 2. The comparison between the traditional GVF method and our approach for their behaviors on the boundary concavity and boundary gap

Definition: A point is called *source* if none of its neighbors points to it. In other words, a point A is a *source* if and only if, for any neighbor B of A:

$$\vec{v}_B \cdot \vec{BA} \le 0,$$

where $\vec{v}_B$ is the diffused gradient vector at B and $\vec{BA}$ is the vector from B to A.

3.2. Initial Segmentation and Region Merging

After we identify all seed points, then we can let the initial snakes start to move with the external force that is determined by the previously generated vector field. Then an initial segmentation is obtained over the image domain. Remember that we use multiple snakes in our algorithm to reduce the dependence on the choice of parameters, like the dual active snake seen in [12]. After the initial segmentation we use region merging technique [13] to further improve the segmentation results.

It is beneficial to take a look at the relationship between the well-known *watershed* method (see [14, 13]) and our method. The *watershed* method begins with the image gradient map and takes the minima of this map as the seeds. A geodesic distance transformation is usually used to obtain the "influence zone", making this approach quite complicated to implement [14]. In our approach, however, it is straightforward to implement initial segmentation based on the gradient vector field. Furthermore, the *watershed* method is sensitive to the noises so that some

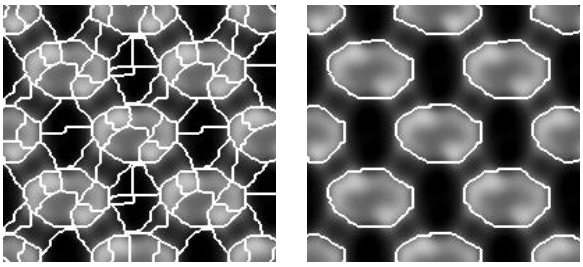

(a) Initial segmentation (b) After region merging

Figure 3. Image segmentation (example I)

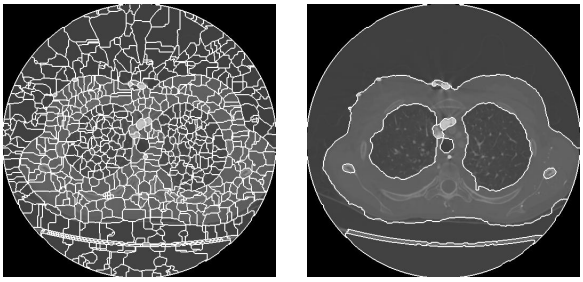

(a) Initial segmentation (b) After region merging

Figure 4. Image segmentation (example II)

kind of smoothing filters must be used before we apply this method. However, our gradient vector diffusion can generate the vector field while smoothing it.

4. Results

In the following we will give some examples of image segmentation by our GVD-based region merging approach. *Fig.3* shows an example of microscopy images. The initial segmentation produces 100 regions (as seen in *(a)*) and after region merging only 14 regions, including one background region, are remained. Although the original image is quite blurred, the cells are still correctly segmented. *Fig.4* shows an example of medical images. There are 688 regions left after initial segmentation, and 16 regions left after region merging. In this example we can see that the most significant features are preserved while the noises are ignored.

5. Conclusion

This paper proposed a new type of diffusion equations to generate *Gradient Vector Field*. We diffused the vectors based on their polar coordinate representations instead of traditional Cartesian coordinate representations. The experiments show that our new approach not only can remedy the problems that traditional snake models have, but also can solve the problems of long-thin boundary concavities and boundary gaps as seen in traditional GVF methods.

References

[1] M. Kass, A. Witkin and D.Terzopoulos, "Snake: Active contour model", *Int. J. Computer Vision*, Vol. 1, pp. 321-331, 1987.

[2] C. Xu and J.L.Prince, "Snakes, Shapes, and Gradient Vector Flow", *IEEE Trans. Image Processing*, Vol. 7, No. 3, pp. 359-369, 1998.

[3] L.D.Cohen and I.Cohen, "Finite-element method for active contour models and balloons for 2D and 3D images", *IEEE Trans. on Pattern Analysis and Machine Intelligence*, Vol. 15, No. 11, pp. 1131-1147, 1993.

[4] C. Xu and J.L.Prince, "Generalized gradient vector flow external force for active contour", *Signal Processing - An International Journal*, Vol. 71, No. 2, pp. 131-139, 1998.

[5] C. Xu and J. L. Prince, "Gradient Vector Flow Deformable Models", *Handbook of Medical Imaging, edited by Isaac Bankman, Academic Press*, September, 2000.

[6] B.Leroy, I.Herliin, and L.D.Cohen, "Multi-resolution algorithm for active contour models", *In 12th Int. Conf. Analysis and Optimization of System*, pp. 58-65, 1996.

[7] L.D.Cohen, "On active contour models and balloons, *CVGIP: Image Understanding*, Vol. 53, pp. 211-218, March 1991.

[8] P.Perona and J.Malik, "Scale-space and edge detection using anisotropic diffusion", *IEEE Trans. on Pattern Analysis and Machine Intelligence*, Vol. 12, No. 7, pp. 629-639, 1990.

[9] J. Shah, "A common framework for curve evolution, segmentation and anisotropic diffusion", *in Proceedings of International Conference on Computer Vision and Pattern Recognition: CVPR'96*, pp. 136-142, June 1996.

[10] D.Geiger, A.Gupta, L.A.Costa and J.Vlontzos, "Dynamical programming for detecting, tracking and matching deformable contours", *IEEE Trans. on Pattern Analysis and Machine Intelligence*, Vol. 17, No. 3, pp. 294-302, 1995.

[11] G.Storvik, "A Bayesian approach to dynamic contours through stochastic sampling and simulated annealing", *IEEE Trans. on Pattern Analysis and Machine Intelligence*, Vol. 16, No. 10, pp. 976-986, 1994.

[12] S.R.Gunn and M.S.Nixon, "Robust snake implementation: a dual active contour", *IEEE Trans. on Pattern Analysis and Machine Intelligence*, Vol. 19, No. 1, pp. 63-67, 1997.

[13] K.Haris, S.N.Efstratiadis, N.Maglaveras and A.K.Katsaggelos, "Hybrid Image Segmentation Using Watersheds and Fast Region Merging", *IEEE Trans. on Image Processing*, Vol. 7, No. 12, pp. 1684-1699, 1998

[14] L.Vincent and P.Soille, "Watersheds in Digital Spaces: An Efficient Algorithm Based on Immersion Simulations", *IEEE Trans. on Pattern Analysis and Machine Intelligence*, Vol.13, No. 6, pp. 583-598, 1991